MRS Communications (2015), *5*, 205–210
doi:10.1557/mrc.2015.29

MRS Communications

Polymers/Soft Matter Research Letter

Enhancing dielectric breakdown strength: structural relaxation of amorphous polymers and nanocomposites

Christopher A. Grabowski, Materials and Manufacturing Directorate, Air Force Research Laboratory, Wright Patterson Air Force Base, Ohio 45433; UES, Inc., Dayton, Ohio 45432, USA
Hilmar Koerner and **Richard A. Vaia,** Materials and Manufacturing Directorate, Air Force Research Laboratory, Wright Patterson Air Force Base, Ohio 45433, USA

Address all correspondence to Richard A. Vaia at **richard.vaia@us.af.mil**

(Received 3 March 2015; accepted 28 April 2015)

Abstract

The thermal history of amorphous polymers near the glass-transition temperature determines the extent to which macromolecules structurally relax, and ultimately their properties. Here, we report the correlation between physical aging, dielectric breakdown, and capacitive energy storage of polystyrene, poly(methyl-methacrylate), and associated silica nanocomposites. Guided by enthalphic recovery rates, dielectric breakdown strength increased from 20% to 40% when aged at T_g−10 °C before use. The generality of improvement and connection to enthalpic recovery afford a means to design pre-service processing of new polymers and additive manufacturing techniques to reduce excess volume within the glass; and thereby reduce initiation and inhibit propagation of electronic failure.

Simultaneously improving the power and energy density of electrostatic capacitors, and decreasing the size of the power subsystem, is critical for advancing medical, transportation, and aerospace technologies.[1] Furthermore, the rapid emergence of flexible hybrid electronics and printing technologies promises to integrate passives into the device package and eliminate surface-mounted components. To maximize theoretical energy storage density ($=1/2\varepsilon_o\varepsilon_r|E_{BD}|^2$), the relative permittivity ε_r and breakdown strength E_{BD} must be concurrently increased by approaches that optimize new materials with new processing techniques. Although amorphous polymers have relatively low ε_r, their high breakdown strength, ease of processability, and affordability offer practical advantages over pure ceramics, and thus are the current choice for many emerging applications and manufacturing technologies. The addition of inorganic nanoparticles with substantially higher ε_r conceptually affords a means to increase permittivity while maintaining the polymeric characteristics that are key to scalability.[2] In concert with these material innovations, processing is just as critical to maximize energy storage. In addition to purification, protocols must avoid trapped solvent and voids. Such defects serve as initiation sites for premature breakdown, and lower the effective dielectric strength.[3] The relation between this "free-volume" and dielectric breakdown strength has been established; for example by experiments on amorphous copolymers[4] and through percolation theory simulations.[5] Initiation of breakdown within a polymer is associated with the largest voids,[6] and has been used to explain numerous observations, such as the relationship between polymer density, composition and breakdown, and the decrease in breakdown strength as service temperature approaches T_g.[4,6] However, processing procedures reported in literature and practiced in industry vary widely, with minimal relationship to the physics underlying the generation of this "free-volume", such as gelation, vitrification, and structural relaxation. Rather these procedures have been developed empirically for a specific material through extensive testing. For example, residual solvent is nominally driven from the film at an empirically chosen temperature and vacuum; followed by a treatment above the glass-transition temperature, T_g.[7,8] Likewise for semi-crystalline polymers such as biaxial oriented polypropylene, anneals above T_g are used to optimize the crystallite morphology. In both cases though, the subsequent cooling procedure to room temperature is rarely discussed. The cooling rate however is what determines the excess thermodynamic properties (i.e., volume, enthalpy, and entropy) of the amorphous polymer, and its relationship to an equilibrium glass.[9,10] Thus, can pre-service processing procedures be prescribed based on the physics underlying the generation and evolution of the excess thermodynamic properties within a quenched polymer? For example, to what extent can capacitive performance be improved by purposeful structural relaxation within the glass?

Structural relaxation (physical aging) impacts mechanical and optical properties of amorphous polymers[11]; however, understanding its impact on dielectric performance and failure has seen little investigation.While investigating in-service failures, Vouyovitch et al. reported breakdown strength improvements up to 25%–40% after annealing inorganic-filled epoxies at

T_g−18 °C.[12] In these composites, improvements were first observed after 2 weeks of such treatment, and required as much as 2 months before breakdown strength was maximized. Champion and Dodd studied the electrical tree growth of unfilled epoxy resins and found breakdown pathways became more fractal in nature as the material was stored at room temperature, reflecting a more tortuous pathway for the discharge cascade.[13] These improvements were attributed to a densification of the resin matrix, but correlating the relative contribution from reduction in excess volume or reduction of unsaturated network bonds could not be ascertained due to the lack of direct measurement of excess thermodynamic properties.

In this study, we investigate the impact of structural relaxation on capacitive energy storage in amorphous polystyrene (PS), polymethyl methacrylate (PMMA), and their corresponding blended and single-component nanocomposites with silica. PS is non-polar with relatively poor breakdown strength (400 V/μm) and low dielectric loss ($\varepsilon'' \sim 10^{-3}$ at 1 kHz), whereas PMMA is polar with excellent breakdown strength and high dielectric loss (800 V/μm and $\varepsilon'' \approx 10^{-1}$ at 1 kHz, respectively). The dielectric breakdown strength, permittivity, loss tangent, and energy storage are compared for films annealed below T_g after quenching from the melt. For example, annealing at T_g−10 °C for 3–12 h enhances the effective breakdown strength of PS and PMMA films by up to 35% and nanocomposites by up to 45%. Most importantly, the anneal temperature and rate of improvement are comparable with prior reports of structural recovery (enthalpy and volume) of PS, which reaches equilibrium after ∼1 day at T_g−9 °C.[14,15]

Figure 1 summarizes structural relaxation in amorphous polymers, as well as providing representative examples of the polymer nanocomposites examined. The extent that the molecular structure of a glass deviates from its ideal equilibrium depends on the cooling rate from the melt (i.e., faster cooling rate equates to greater deviation, Fig. 1a). Structural relaxation refers to the molecular level processes that evolve the excess thermodynamic properties (e.g., volume and enthalpy) of the cooled non-equilibrium glass toward the melt-extrapolated equilibrium state. The sub-T_g anneals and resultant changes in physical properties are referred to as physical aging.[11] Note that here the glass-transition temperature, T_g, reflects rapid cooling from the melt to ensure consistency with thermal history and physical aging discussions. Table I summarizes the relevant characteristics of the materials discussed.[8] In addition to unfilled PS and PMMA (Polymer Source; M_w = 100 and 88 kg/mol, respectively), traditional blended polymer nanocomposites, Fig. 1b, and assemblies of matrix-free hairy silica nanoparticles (aHNPs),[13] Fig. 1c, are also examined. The blended nanocomposites and aHNPs were synthesized and prepared following Refs 16 and 17, respectively. The silica is well dispersed at all volume fractions, as discussed in prior morphology-processing studies.[18] A more ordered morphology is observed in the aHNP films due to the covalent grafting of the polymer chains to the silica surface, which establishes a finite minimum particle–particle separation.[16,18] All materials were purified to electronic-grade standard by dissolution in methyl ethyl ketone, passing through a silica gel column, precipitation in methanol, and drying in a rotary evaporator (see Supporting Information).

Figure 2 compares the characteristic breakdown strength of neat PS and PMMA films (3 μm thick) aged for increasing times, t_a, at T_g-10 °C after a 30 °C/s quench from an initial 24 h vacuum anneal at T_g + 25 °C. Dielectric failure data (Fig. 2a for PS and Supporting Information Fig. S1 for PMMA) were fit to a two-parameter Weibull cumulative probability function, $P(E)=1-\exp[-(E/E_{BD})^{\beta}]$, where $P(E)$ is the cumulative probability for failure, E is the experimental breakdown strength, E_{BD} represents the electric field for which there is 63.2% probability for failure (Fig. 2b), and β is the shape parameter associated with the least-squares fit of the distribution (Fig. 2c). Error bars represent one standard deviation within the breakdown data. For PS and PMMA, E_{BD} initially increases from 420 and 805 V/μm at $t_a = 0$, to a plateau of approximately 570 and 970 V/μm for $t_a > 3$ h. In concert, β increases, reflecting a commensurate narrowing of the distribution of the breakdown values. This narrowing however preferentially occurs at the low value side of the distribution (Fig. 2a and Fig. S1). Dielectric failure of glassy polymers occur due to extrinsic factors (such as chemical impurities and trapped solvent), and the inherent microstructural variations and density fluctuations within the polymer matrix.[19] Using electronic-grade polymers and thoroughly annealing solvent-cast polymer films at $T > T_g$, we limit the influence of the extrinsic impurities. As a polymer glass evolves toward equilibrium, structural relaxation processes reduce the magnitude and spatial frequency of local density fluctuations, thus minimizing structural variability.[9] The increased dielectric strength associated with physical aging therefore appears to reflect a reduction of the number density of largest flaws that are associated with the initiation and propagation of breakdown.

The rate at which this improvement in dielectric strength occurs is consistent with reported enthalpy loss measurements. The recovery of excess volume and enthalpy in a polymer glass follows the Vogel–Fulcher–Tammann (VFT) relationship and recent studies indicate that enthalpy and volume recover at comparable rates.[20] Thus enthalpy recovery experiments provide insight into volume recovery in a polymer glasses. For neat PS, complete enthalpic recovery occurs in ∼80 and 500 h at T_g−9 °C (91 °C) and T_g−10 °C (90 °C), respectively.[14] Furthermore, due to its power-law dependence, over 85% of the recovery occurs in 12 h at 91 °C. This is qualitatively consistent with maximum breakdown occurring for $t_a \sim 11$ h at 90 °C, especially considering the larger temperature variation in laboratory ovens (±2–3 °C, Fisher Scientific 282A vacuum oven), compared with controlled differential scanning calorimetry (DSC) experiments.

Figure 3 summarizes the extent to which physical aging may also improve the dielectric breakdown of polymer nanocomposites (see Table I for sample identification and T_g information). Note that the reported impact of silica loading and nanocomposite

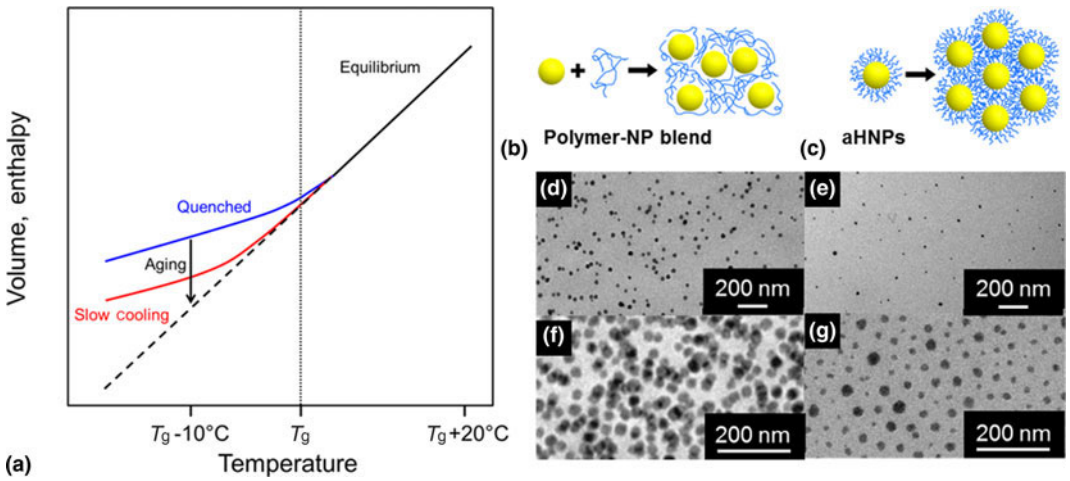

Figure 1. (a) Diagram illustrating the change in volume and enthalpy for amorphous polymers during structural relaxation below the glass transition. Here, T_g refers to the glass-transition temperature recorded upon cooling. (b, c) Illustrations of nanocomposites: a traditional polymer–nanoparticle blend and a matrix-free aHNPs, respectively. Representative transmission electron microscopy (TEM) images of PMMA silica nanocomposite films: (d) blend 1% v/v loading, (e) aHNP 0.7% v/v, (f) blend 15% v/v, and (g) aHNP 16% v/v. Blend films are 90 nm thick microtome slices, whereas aHNP are a monolayer thick formed from toluene solution drop cast onto a carbon-coated copper grid.

architecture on T_g is consistent with prior reports for PS– and PMMA–silica blends as well as hnp–PMMA and hnp–PS.[21,22] Recent studies by Boucher et al. showed accelerated structural relaxation for blended PMMA–silica nanocomposites, whereas no change in the enthalpy recovery rate was observed for blended PS–silica nanocomposites.[23] aHNPs exhibit similar rate behavior to their blended analogs.[24] Therefore, to consider the maximum effect of physical aging, we compare dielectric breakdown, E_{BD}, for $t_a = 0$ and 24 h at T_g–10 °C. Overall, E_{BD} at $t_a = 0$ decreases with silica loading in PMMA and is relatively insensitive to silica loading in PS. These data are consistent with prior reports where the impact of uniformly disperse silica on breakdown reflected the relative polarity of the silica surface to the surrounding matrix.[25] The more polar silica likely behaves as a trap or scattering site in the less polar PS, whereas it behaves as a defect in the even more polar PMMA. Upon aging for $t_a = 24$ h, E_{BD} increases irrespective of the type of nanocomposite for low-to-intermediate silica

Table I. Composition and thermal properties for polymer, traditional blended, and matrix-free hairy (polymer grafted) nanoparticle nanocomposites.

Sample[a]	SiO_2 fraction (% v/v)	Degree of polymerization	Graft density (chains/nm^2)	T_g (°C)[b]
PMMA	0	880	–	110
PS	0	960	–	99
hnp–PMMA-8	7.9	650	0.27	115
hnp–PMMA-16	16.3	390	0.20	110
hnp–PMMA-48	48.0	200	0.08	115
hnp–PS-18	18.1	100	0.61	98
blend–PMMA-7.5	7.5	3100	–	112
blend–PMMA-15	15.0	3100	–	114
blend–PMMA-30	30.0	3100	–	115
blend–PS-15	15.0	5500	–	102

[a]PMMA, polymethyl methacrylate; PS, polystyrene; hnp-*x*-*y*, matrix-free hairy nanoparticle nanocomposite with *x*-polymer graft and *y* v/v% silica. blend-*x*-*y*: traditional blended nanocomposite with *x*-polymer matrix and *y* v/v% silica.

[b]T_g values are obtained from the average of 2–3 DSC cooling cycles. Uncertainty in T_g measurements is ±3%.

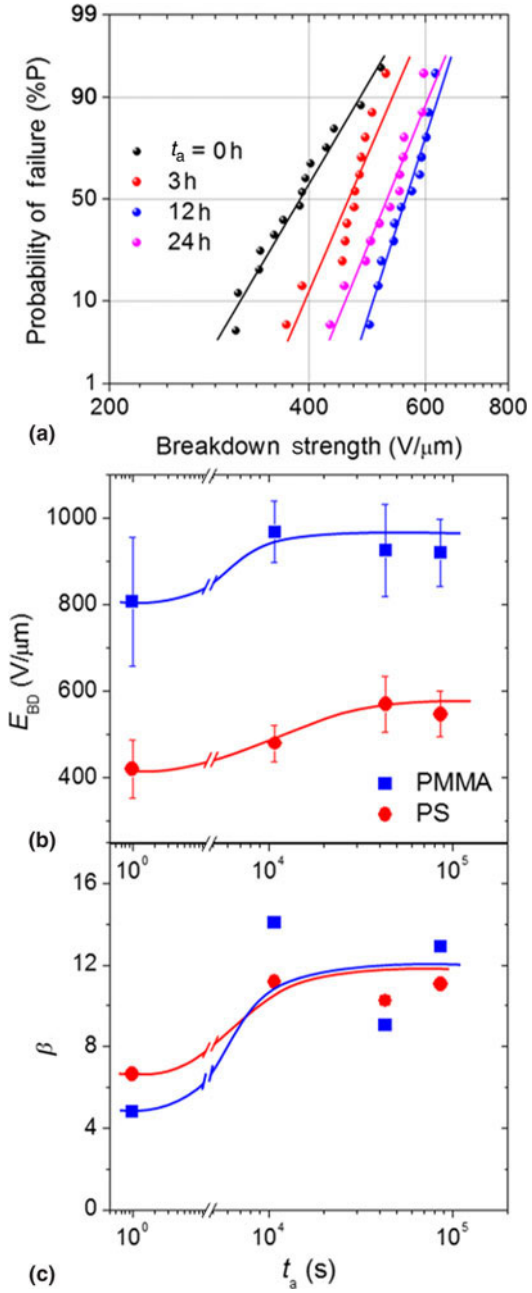

Figure 2. (a) Probability of failure for PS (100 kg/mol M_w) films aged at t_a = 0, 3, 12, and 24 h. Lines correspond to two-parameter Weibull fittings. Corresponding PMMA (88 kg/mol M_w) Weibull plots are available in Supporting Information. (b, c) Characteristic breakdown strength and Weibull parameter β for PS (red circles) and PMMA (blue squares) measured after aging for a duration of t_a at T_g−10 °C, respectively. Samples were quenched at 30 °C/s. Lines provide a guide to data trends.

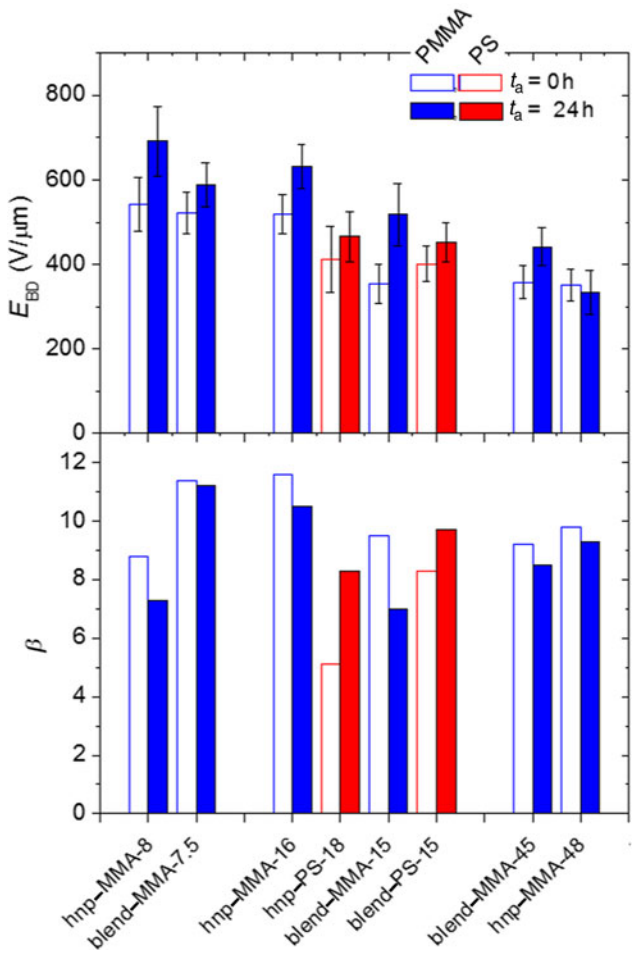

Figure 3. (top) Characteristic breakdown strength, E_{BD}, for representative PS and PMMA nanocomposite films measured after t_a = 0 and 24 h at T_g−10 °C (blue and red, respectively). (bottom) Corresponding Weibull parameter β. T_g and sample identification are listed in Table I.

loadings (<20% v/v). For example, the E_{BD} of hnp–PMMA-8 (80 kg/mol M_w, 0.27 chains/nm^2 graft density) increases from 543 to 691 V/μm. A traditional blend sample with comparable silica loading, blend–PMMA-7.5, shows an increase from 521 to 589 V/μm. The Weibull parameter β values fall within a narrow range, between 7 and 11, irrespective of aging. This indicates that the improvement in nanocomposite E_{BD} with aging is more likely associated with overall densification than any preferential elimination of large density fluctuations.

The consistency of E_{BD} enhancement over such a broad range of silica volume fraction, polymer–nanoparticle interface, and matrix chemistry confirms the underlying mechanism for these enhancements is related to the general characteristics of the polymer glass. It is also important to note that the only sample in our investigation that did not show improved breakdown strength after physical aging was hnp–PMMA-48 (25 kg/mol M_w, 0.08 chains/nm^2 graft density). Extreme silica loading, and associated geometrical confinement of the chains, cannot be the sole factor responsible for this deviation since a traditionally blended PMMA nanocomposite with comparable silica loading (45% v/v) did show ~20% enhanced E_{BD}. Rather, it seems that the combination of polymer tethering with geometrical confinement limits this structural relaxation of the nanocomposite. This is consistent with recent enthalpy relaxation experiments of

blended and aHNP nanocomposites, which show significantly reduced enthalpy relaxation in high silica content aHNPs comprised of low-graft density, high molecular weight, hairy nanoparticles.[24]

To assess the complete impact of physical aging on energy storage, permittivity, loss tangent, and D–E polarization loops were measured for select samples (see Supporting Information). Overall, the permittivity of the quenched PS and PMMA are consistent with prior studies, and that of the nanocomposites follow effective medium models, such as the Bruggeman model, with increasing silica ($\varepsilon \approx 3.9$) content.[18] Physical aging in general did not substantially impact the permittivity or loss tangent. Both blended and aHNP nanocomposites although did exhibit slight increases in permittivity (5%–10%) (Figs S2 and S3), which may reflect an initially more open glass structure upon cooling due to the silica, and thus a measurable increase in dipole density due to polymer densification during the annealing. Concurrently, the loss tangent also slightly decreased at low frequencies. This is also consistent with densification inhibiting mobility and transport.

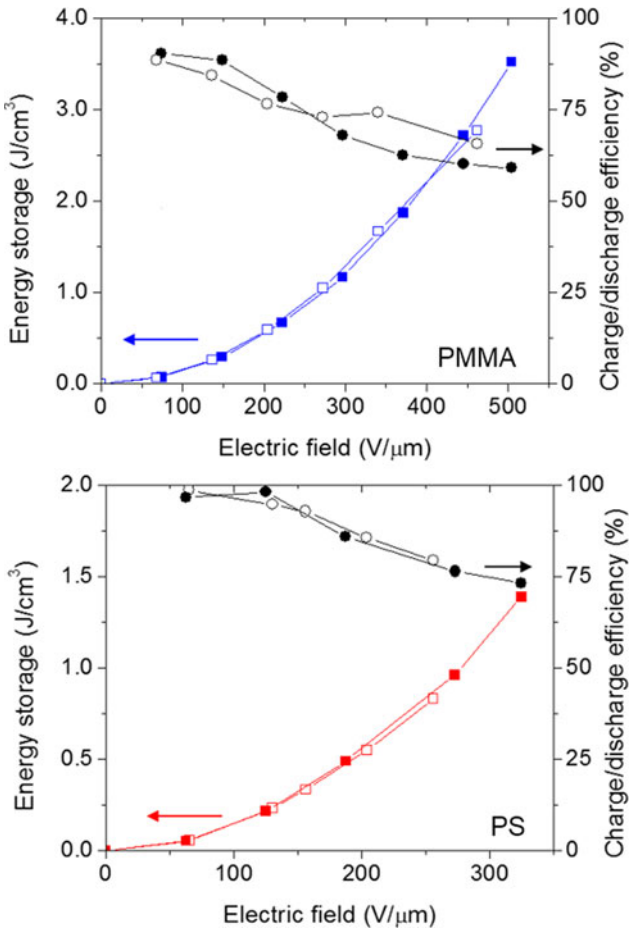

Figure 4. Recovered energy density and charge/discharge efficiency while increasing applied electric field for PMMA (top) and PS (bottom) after aging at $T_g - T = 10$ °C for $t_a = 0$ (open) and 24 h (closed).

Charge/discharge efficiency for representative polymer and nanocomposties are summarized in Fig. 4 and Fig. S6. Detailed D–E polarization loops may be found in the Supporting Information Figs S4 and S5. Since the dielectric characteristics are effectively unchanged by physical aging, the increased capacitive performance arises from the improved dielectric breakdown characteristics. The increased E_{BD} and narrower distribution leads to the ability to drive a capacitor to higher fields and thus realize a higher practical energy storage. PMMA delivers 3.5 J/cm^3 at 500 V/μm, and PS delivers 1.4 J/cm^3 at 325 V/μm after aging for 24 h. Samples not subjected to aging failed at these elevated electric fields. Aging of blend nanocomposites (blend–PS-15 and blend–PMMA-15) resulted in a substantial improvement of efficiency at high (>200 V/μm) fields, from <50–60% to >75% (Fig S6). This may be related to the reduced transport arising from densification upon structural relaxation of the polymer glass. A table summarizing the overall capacitive performance may be found in the Supporting Information, Table S1.

In conclusion, this study has shown that structural relaxation within a polymer glass increases the mean dielectric breakdown strength as well as preferentially reducing the probability of failure below the mean value. This results in an increase in the maximum electric field applied in-service. The effect is general, occurring for different polymer chemistries (PS and PMMA) and for many different nanocomposite variations (i.e., silica loading, blended, and aHNPs). Most importantly, the rate of enhancement across all these systems is consistent with available enthalpy recovery studies—motivating future investigation of the structural recovery rate of potential dielectric polymers and nanocomposites. Correlations between fundamental thermodynamic characteristics of the polymer and processing protocols will enhance the speed at which new materials and manufacturing technologies can be optimized for capacitive energy storage.

Supplementary materials

For supplementary material for this article, please visit http://dx.doi.org/10.1557/mrc.2015.29

Acknowledgments

The authors thank the Air Force Office of Scientific Research and Air Force Research Laboratory Materials & Manufacturing Directorate for their financial support along with V. McNeir and J. DeCerbo for their assistance with energy storage characterization, and C. Chi (Dupont de Nemours & Co.) for colloidal silica samples. The authors also thank the Bockstaller and Matyjaszewski groups (Carnegie Mellon University) and J. S. Meth (DuPont) for supplying nanocomposite samples and images.

References

1. Z.M. Dang, J.K. Yuan, S.H. Yao, and R.J. Liao: Flexible nanodielectric materials with high permittivity for power energy storage. *Adv. Mater.* **25**, 6334–6365 (2013).

2. Q. Wang and L. Zhu: Polymer nanocomposites for electrical energy storage. *J. Polym. Sci. B, Polym. Phys.* **49**, 1421–1429 (2011).
3. L.A. Dissadio and J.C. Fothergill: *Electrical Degradation and Breakdown in Polymers* (Peter Peregrinius Ltd., London, UK, 1992) pp. 601.
4. H. Sabuni and J.K. Nelson: The electric strength of copolymers. *J. Mater. Sci.* **12**, 2435–2440 (1977).
5. K. Wu, T. Okamoto, and Y. Suzuoki: Simulation study on the correlation between morphology and electrical breakdown in polyethylene. *J. Appl. Phys.* **98**, 114102 (2005).
6. J. Artbauer: Electric strength of polymers. *J. Phys. D, Appl. Phys.* **29**, 446–456 (1996).
7. S.A. Paniagua, Y. Kim, K. Henry, R. Kumar, J.W. Perry, and S.R. Marder: Surface-initiated polymerization from barium titanate nanoparticles for hybrid dielectric capacitors. *ACS Appl. Mater. Interface.* **6**, 3477–3482 (2014).
8. J. Li, J. Claude, L.E. Norena-Franco, S.I. Seok, and Q. Wang: Electrical energy storage in ferroelectric polymer nanocomposites containing surface-functionalizedBaTiO3 nanoparticles. *Chem. Mater.* **20**, 6304–6306 (2008).
9. J.M. Hutchinson: Physical aging of polymers. *Prog. Polym. Sci.* **20**, 703–760 (1995).
10. D. Cangialosi, V.M. Boucher, A. Alegria, and J. Colmenero: Physical aging in polymers and polymer nanocomposites: recent results and open questions. *Soft Matter* **9**, 8619–8630 (2013).
11. R.D. Priestley: Physical aging of confined glasses. *Soft Matter* **5**, 919–926 (2009).
12. L. Vouyovitch, N.D. Alberola, L. Flandin, A. Beroual, and J.-L. Bessede: Dielectric breakdown of epoxy-based composites: relative influence of physical and chemical aging. *IEEE Trans. Dielectr. Electr. Insul.* **13**, 282–292 (2006).
13. J.V. Champion and S.J. Dodd: The effect of voltage and material age on the electrical tree growth and breakdown characteristics of epoxy resins. *J. Phys. D, Appl. Phys.* **28**, 398–407 (1995).
14. Y.P. Koh and S.L. Simon: Enthalpy recovery of polystyrene: does a long-term aging plateau exist? *Macromolecules* **46**, 5815–5821 (2013).
15. S.L. Simon, J.W. Sobieski, and D.J. Plazek: Volume and enthalpy recovery of polystyrene. *Polymer* **42**, 2555–2567 (2001).
16. J.S. Meth, S.G. Zane, C.Z. Chi, J.D. Londono, B.A. Wood, P. Cotts, M. Keating, W. Guise, and S. Weigand: Development of filler structure in colloidal silica-polymer nanocomposites. *Macromolecules* **44**, 8301–8313 (2011).
17. J. Pietrasik, C.M. Hui, W. Chaladaj, H. Dong, J. Choi, J. Jurczak, M.R. Bockstaller, and K. Matyjaszewski: Silica-polymethacrylate hybrid particles synthesized using high-pressure atom transfer radical polymerization. *Macromol. Rapid Commun.* **32**, 295–311 (2011).
18. C.A. Grabowski, H. Koerner, J.S. Meth, A. Dang, C.M. Hui, K. Matyjaszewski, M.R. Bockstaller, M.F. Durstock, and R.A. Vaia: Performance of dielectric nanocomposites: matrix-free, hairy nanoparticle assemblies and amorphous polymer-nanocomposite blends. *ACS Appl. Mater. Interfaces* **6**, 21500–21509 (2014).
19. Y. Sun, S.A. Boggs, and R. Ramprasad: The intrinsic electric breakdown strength of insulators from first principles. *Appl. Phys. Lett.* **101**, 132906 (2012).
20. P. Badrinarayanan and S.L. Simon: Origin of the divergence of the timescales for volume and enthalpy recovery. *Polymer* **48**, 1464–1470 (2007).
21. M.N. Tchoul, S.P. Fillery, H. Koerner, L.F. Drummy, F.T. Oyerokun, P.A. Mirau, M.F. Durstock, and R.A. Vaia: Assemblies of titanium dioxide-polystyrene hybrid nanoparticles for dielectric applications. *Chem. Mater.* **22**, 1749–1759 (2010).
22. P. Rittigstein and J.M. Torkelson: Polymer-nanoparticle interfacial interactions in polymer nanocomposites: confinement effects on glass transition temperature and suppression of physical aging. *J. Polym. Sci. B, Polym. Phys.* **4**, 2935–2943 (2006).
23. V.M. Boucher, D. Cangialosi, A. Alegria, and J. Colmenero: Physical aging in PMMA/silica nanocomposites: enthalpy and dielectric relaxation. *J. Non-Cryst. Solids* **357**, 605–609 (2011).
24. H. Koerner, M.R. Bockstaller, A. Dang, C. Mahoney, K. Matyjaszewski, C.M. Hui, and R.A. Vaia: Physical aging within hairy nanoparticle assemblies. *Bull. Am. Phys. Soc.* **59** (2014).
25. C.A. Grabowski, S.P. Fillery, N.M. Westing, C. Chi, J.S. Meth, M.F. Durstock, and R.A. Vaia: Dielectric breakdown in silica–amorphous polymer nanocomposite films: the role of the polymer matrix. *ACS Appl. Mater. Interface.* **5**, 5486–5492 (2013).